

and R. C. M. de Groot for their assistance with X-ray data collection and magnetic measurements, respectively.

Registry No. 1, 98758-75-9; 2, 98720-88-8; 3, 98759-90-1; 4, 98720-89-9.

Supplementary Material Available: Listings of observed and calculated structure factors, fractional atomic coordinates and isotropic thermal parameters for the hydrogen atoms, anisotropic thermal parameters for the non-hydrogen atoms, and further bond distances and angles (15 pages). Ordering information is given on any current masthead page.

Contribution from the Laboratoire de Physico-Chimie Moléculaire, UA 474, Institut Universitaire de Recherche Scientifique, 64000 Pau, France, and Laboratoire CNRS-SNPE, 94320 Thiais, France

Stabilization of Phosphinidene and Phosphirene by Complexation on Phosphorus. Theoretical Studies and Photoelectron Spectra[†]

D. GONBEAU,[‡] G. PFISTER-GUILLOUZO,*[‡] A. MARINETTI,[§] and F. MATHEY[§]

Received December 7, 1984

Electronic structures of phosphinidene and phosphirene complexes are described, extended Hückel theory, ab initio calculations, and data from UV photoelectron spectroscopy in conjunction. The nature of the metal-phosphorus double bond in these compounds was investigated. The stabilization of phosphinidene and phosphirene by complexation on phosphorus was studied on the basis of the diagram of orbital correlation with the fragment orbitals. These conclusions agree with analysis of photoelectron spectra of stable phosphirene complexes.

The chemistry of phosphinidene complexes has been extensively studied by two of us.² A similarity between the behavior of terminal complexes of phosphinidene and that of singlet carbene was suggested.

The present report is a quantum-chemical examination of this entity. The nature and the electronic origin of the M-P bonds (M = Cr, Fe) were first analyzed on the basis of a diagram of orbital interactions between the different orbitals of the fragments, obtained from extended Hückel theory (EHT) calculations. This method, previously used with success for the study of Fischer type carbene complexes³ of Schrock complexes,⁴ does not lead to a rigorous determination of spin states. For this reason, we carried out a more sophisticated PSHONDO ab initio calculation⁵ on pentacarbonyl(phosphinidene)chromium. Various results⁶ have shown that this formalism generates results comparable to those of "all electrons" SCF calculations.

In parallel to the data it supplied on the electronic structure of complexed phosphinidene, this approach was used as the basis for studying the system of complexed phosphirene, the only stable compound isolated. The photoelectron spectra of a number of derivatives of the latter compound were analyzed in order to utilize these experimental data to verify the coherency of conclusions drawn from the quantum-chemical study.

Computational and Experimental Details

EHT calculations were performed with the parameters previously utilized⁴ for Cr and Fe.

All SCF calculations were carried out with use of version of the HONDO program PSHONDO.

For carbon, oxygen, and phosphorus the pseudopotentials and basis sets chosen were those previously determined.⁷ The four Gaussian functions were contracted to the double- ζ level (3 + 1) for each atom except for carbon and oxygen in Cr(CO)₅, which were treated at the single- ζ level, because of the considerable computing effort in the case of the phosphirene complex. For phosphorus, a 3d Gaussian was added ($\alpha_d = 0.57$) as a polarization function.

We have determined the nonempirical atomic pseudopotential for chromium from the atomic Hartree-Fock calculations of Clementi and Roetti.⁸ A valence basis set (4s,4p,3d) was optimized for this atom in a pseudopotential SCF calculation of the atomic ground state, with use of a basis set previously proposed.⁹ For 4s and 3d orbitals these Gaussian functions were contracted to the double- ζ level by means of a 2 + 1 procedure for 4s and 4 + 1 for 3d.

The Gaussian valence basis set and pseudopotentials are described in Tables I and II.¹⁰

The SCF valence energies for the open-shell triplet states were obtained by calculating the mean value of the H operator between the wave functions, determined from a Nesbet type operator.¹¹

According to Koopmans' theorem (KT) the mono-electronic levels are related to ionization potentials (IP's). However, KT IP's do not take into account polarization and correlation effects. The following procedure¹² was used to estimate the corrections (to KT values) required to reach more realistic IP's. Polarization of the positive ion is approximated by first-order perturbation theory as

$$\Delta\epsilon_k(\text{pol}) = \sum_{ij^*} \frac{\langle i|F_k^+|j^*\rangle^2}{\epsilon_i - \epsilon_{j^*}}$$

where F_k^+ is the Fock operator obtained after removal of one electron from orbital k and i and j^* are the SCF molecular orbitals of the neutral molecule. The main part of correlation decrease in the positive ion is due to the lack of double excitations from orbital k and can be approximated by

$$\Delta\epsilon_k(\text{cor}) = \sum_{j^*l^*} \frac{\langle kj^*|kl^*\rangle^2}{2\epsilon_k - \epsilon_{j^*} - \epsilon_{l^*}}$$

Both contributions are easy to evaluate and require a computing effort equivalent to only one SCF iteration.

- (1) Part 24: Garcia, J. L.; Gonbeau, D.; Pfister-Guillouzo, G.; Roch, M.; Weber, J. *Can. J. Chem.*, in press.
- (2) (a) Marinetti, A.; Mathey, F.; Fischer, J.; Mitschler, A. *J. Chem. Soc., Chem. Commun.* **1982**, 667 (b) Marinetti, A.; Mathey, F.; Fischer, J.; Mitschler, A. *J. Am. Chem. Soc.* **1982**, *104*, 4484 (c) Marinetti, A.; Mathey, F. *Organometallics*, **1984**, *3*, 456.
- (3) Hoffmann, R. *Angew. Chem., Int. Ed. Engl.* **1982**, *21*, 711 and references cited therein.
- (4) Goddard, R. J.; Hoffmann, R.; Jemmis, E. D. *J. Am. Chem. Soc.* **1980**, *102*, 7667.
- (5) (a) Dupuis, M.; Rys, J.; King, H. F. *J. Chem. Phys.* **1976**, *65*, 111. (b) Durand, P.; Barthelat, J. C. *Theor. Chim. Acta* **1975**, *38*, 283.
- (6) (a) Barthelat, J. C.; Durand, P. *Gazz. Chim. Ital.* **1978**, *108*, 225. (b) Dixon, R. N.; Robertson, I. L. *Theor. Chem. (London)* **1978**, *3*, 100.
- (7) Laboratoire de Physique Quantique, Toulouse Ateliers, France (October 1981).
- (8) Clementi, E.; Roetti, C. *At. Data Nucl. Data Tables* **1974**, *14*, 177.
- (9) (a) Wachters, A. J. H. *J. Chem. Phys.* **1970**, *52*, 1033. (b) Rappe, A. K.; Smedley, T. A.; Goddard, W. A. *J. Chem. Phys.* **1981**, *85*, 2607.
- (10) Supplementary material.
- (11) Nesbet, R. K. *Rev. Mod. Phys.* **1963**, *35*, 552.
- (12) (a) Malrieu, J. P. *J. Spectrosc. Photoelectronique* **1978**. (b) Trinquier, G. *J. Am. Chem. Soc.* **1983**, *104*, 6969. (c) Gonbeau, D.; Pfister-Guillouzo, G. *J. Electron. Spectrosc. Relat. Phenom.* **1984**, *33*, 279.

[†] Application of Photoelectron Spectroscopy to Molecular Properties. 25. For Part 24, see ref 1.

[‡] Institut Universitaire de Recherche Scientifique.

[§] Laboratoire CNRS-SNPE.

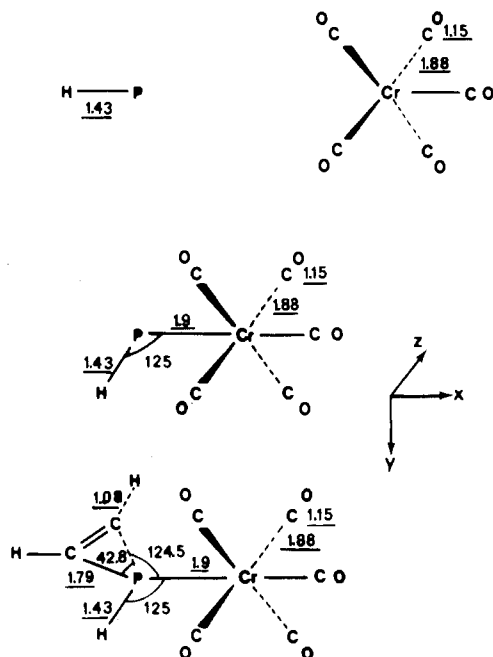


Figure 1. Geometric parameters in PSHONDO (bond lengths in angstroms, angles in degrees).

In terms of geometric parameters of complexed phosphinidenes, P-M lengths and $\angle\text{HPM}$ angles ($M = \text{Fe}, \text{Cr}$) were optimized in EHT (method of successive variations). Thus, P-H was set at 1.43 Å and the structures of the $\text{Cr}(\text{CO})_5$ and $\text{Fe}(\text{CO})_4$ groups were deduced from experimental data obtained with similar compounds, $\text{Cr}(\text{CO})_5(\text{PPh}_3)^{13}$ ($d_{\text{Cr-C}} = 1.88$ Å, $d_{\text{C-O}} = 1.15$ Å) and $\text{Fe}(\text{CO})_5^{14}$ ($d_{\text{Fe-C}} = 1.87$ Å, $d_{\text{C-O}} = 1.15$ Å).

These same geometric parameters were adopted for the PSHONDO calculations, since they were coherent with those obtained with X-ray diffraction of phosphirene complexed with $\text{W}(\text{CO})_5$.^{2b} We chose the data deduced in this latter study for the phosphirene moiety.

The geometries used in PSHONDO are reported in Figure 1.

The compounds have been prepared previously.^{2b}

Spectra were recorded on a PES Laboratories Model 0078 spectrometer equipped with a He I-He II source. All spectra were calibrated with the $2p_{1/2}$ and $2p_{3/2}$ lines of xenon (12.13 and 13.43 eV) and argon (15.76 and 15.93 eV).

Study of Preferential Structures of Phosphinidene Complexes $\text{R-P} \rightarrow \text{ML}_n$ with the EHT Method

We first used the EHT method to analyze the nature and degree of the interactions occurring between a type R-P singlet phosphinidene and a type ML_n metal fragment (hypothesis verified by PSHONDO calculations). This was done in order to estimate the preferential structure of the $\text{R-P} \rightarrow \text{ML}_n$ entities, whose existence was demonstrated by chemical trapping and also by chemical studies.¹⁵

An R-P singlet phosphinidene is characterized by an occupied orbital with p symmetry perpendicular to the R-P bond, " $n_p(\text{P})$ " (donor orbital) and a vacant orbital $p^*(\text{P})$ perpendicular to the plane $n_p(\text{P})$, R-P (acceptor orbital). In comparison to the case for its carbene homologue, this arrangement enables us to a priori predict differences in the interactions that may occur with metallic entities.

In the light of existing experimental results, we successively examined complexing with pentacarbonylchromium and tetracarbonyliron.

Phosphinidene-Chromium Pentacarbonyl Complex. The $\text{Cr}(\text{CO})_5$ fragment derived from the octahedral species $\text{Cr}(\text{CO})_6$ contains three occupied d orbitals, two with π symmetry (d_{xz} and d_{yz} in the Cartesian frame used) and one with $d\delta$ symmetry (d_{xy}). The first virtual orbital has considerable localization on a $d\sigma$ symmetry orbital (d_z).

The primary two-electron stabilizing interactions existing between HP, phosphinidene, and $\text{Cr}(\text{CO})_5$ are shown in Figure 2. They involve $n_p(\text{P})$, the HOMO of the ligand, and the LUMO of $\text{Cr}(\text{CO})_5$, d_z (σ (ligand \rightarrow metal) transfer), and also $p^*(\text{P})$, the LUMO of the ligand, and the d_{yz} HOMO of the metal (π (metal \rightarrow ligand) transfer). Thus they impart a double nature to the P-Cr bond.

The four-electron destabilizing interactions primarily involve $n_p(\text{P})$, σ P-H orbitals, and $d_{xz}(\text{Cr})$. The interactions involving the second lone pair on the phosphorus, energetically very deep, are not determining factors for interpreting the privileged conformation and so were not taken into account.

The most favorable arrangement should a priori be an angle θ of 90° between the H-P and P-Cr bonds, since this would lead to maximal $n_p(\text{P})$, $d_z(\text{Cr})$ overlap. A variation of the main geometric parameters ($d_{\text{P-Cr}}$ and θ) has in fact enabled us to observe that the energetically preferred conformation included $d_{\text{P-Cr}}$ values of 1.9 Å and $\theta = 125^\circ$. In comparison to a value of $\theta = 90^\circ$, the resulting stabilization is considerable, since it is on the order of 92 kJ mol⁻¹.

We also observed that the localization of the H-P bond in the bisecting plane of Cr-CO bonds was favored in relation to an eclipsed H-P Cr-CO position, but only by about 3.3 kJ mol⁻¹. The rotational barrier around the P-Cr bond is thus relatively low, on the same order of magnitude as that determined for $\text{Cr}(\text{CO})_5$ complexed carbenes.¹⁶ It is interesting to note that these results are in good agreement with structural data obtained with X-ray diffraction for complexed phosphirene: $\theta = 125^\circ$ and an R-P bond in the bisecting plane of Cr-CO bonds. The origin of the observed stabilization when the angle θ is opened from 90° to 125° , which decreases $n_p(\text{P})$, $d_z(\text{Cr})$ overlap to a slight extent, is at the level of two factors: (1) There is participation of secondary stabilizing interactions, e.g. $\sigma_{\text{P-H}} \leftrightarrow d_z(\text{Cr})$, and primarily that involving the second virtual orbital with p-d character of the HP fragment (denoted $d^*(\text{P})$) and the d_{xz} orbital of $\text{Cr}(\text{CO})_5$ (zero overlap at 90° , increasing to 0.2 at 125°). For a ligand-metal transfer of the same order, the variation of $\theta = 90^\circ$ - 125° leads to a slightly greater metal-ligand transfer. (2) There is a decrease of destabilizing interactions, shown by an energy decrease of the occupied orbital resulting from the $\sigma_{\text{P-H}} \leftrightarrow d_{xz}(\text{Cr})$ interaction. In reality, this effect reflects steric factors. The stability observed when the dihedral angle formed by the two H-P and Cr-CO bonds passes from 0 to 45° corresponds to a slight increase of the above-mentioned factors.

Phosphinidene-Iron Tetracarbonyl Complex. Two configurations were a priori possible, i.e. the ligand in an axial or equatorial position for the reconstitution of the trigonal bipyramid. We thus carried out calculations for these two conformations.

Optimization of the $d_{\text{P-Fe}}$ bond length and the angle $\angle\text{HPFe}$ furnished similar values in both cases of $d_{\text{P-Fe}} \approx 1.8$ Å and $\angle\text{HPFe} = 120^\circ$. Furthermore, the energetically preferred conformation for an axial ligand involves the P-H bond in the bisecting plane of the Fe-CO bonds. For an equatorial HP ligand we obtained a preferred conformation with the H-P bond in the plane of the axial CO as expected from the analysis of the molecular orbitals of the two fragments separated.

The rotational barrier around the P-Fe bonds in both systems is on the same order of magnitude, about 16.7 kJ mol⁻¹, and is similar to those obtained for carbenes complexed with $\text{Fe}(\text{CO})_4$.¹⁶

Finally, the arrangement of the HP in an equatorial position is favored by about 71.1 kJ mol⁻¹ in comparison to axial orientation. We nonetheless analyzed both types of calculations performed in order to further define the interactions involved.

In the case of an axial ligand, the $\text{Fe}(\text{CO})_4$ fragment presents two pairs of degenerated occupied orbitals and one virtual d_z orbital in the Cartesian frame used. Thus, the primary interactions with phosphinidene involve the $n_p(\text{P})$ HOMO of the latter and the virtual d_z orbital of $\text{Fe}(\text{CO})_4$. In parallel, the metal-ligand transfer occurs via the interaction between the $p^*(\text{P})$ fragment

(13) Carty, A. J.; Taylor, N. J.; Coleman, A. W.; Lappert, M. F. *J. Chem. Soc., Chem. Commun.* **1979**, 639.

(14) Sutton, L. E. *Spec. Publ.-Chem. Soc.* **1958**, No. 11; **1965**, No. 18.

(15) Marinetti, A.; Mathey, F., to be submitted for publication.

(16) Nakatsuji, H.; Ushio, J.; Han, S.; Yonezawa, T. *J. Am. Chem. Soc.* **1983**, *105*, 426.

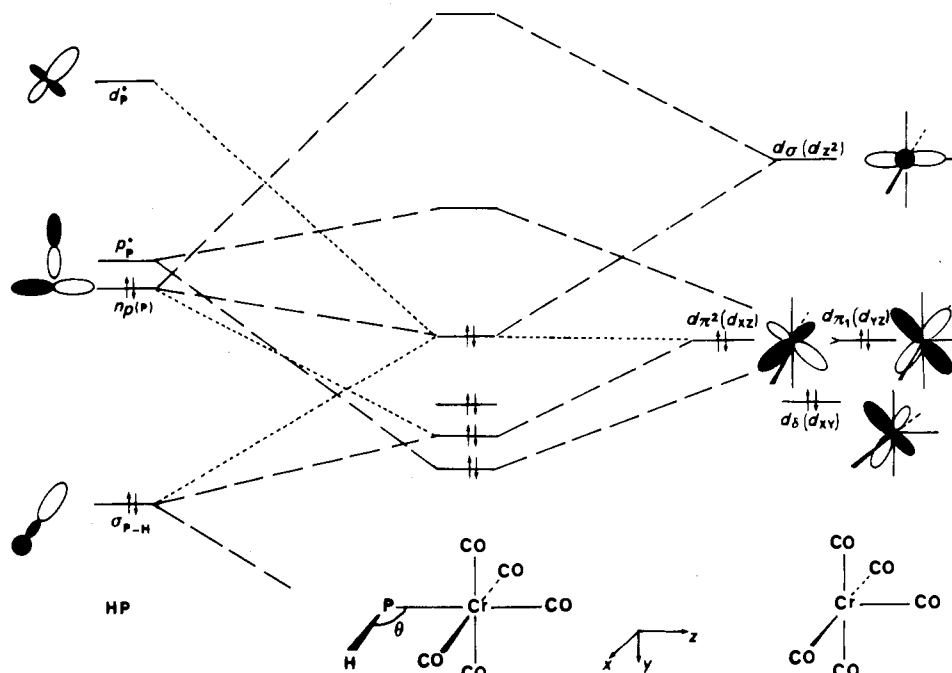


Figure 2. Interaction diagram (EHT) for $\text{HP}=\text{Cr}(\text{CO})_5$ fragments HP, $\text{Cr}(\text{CO})_5$ (conformation eclipsed between $\sigma_{\text{P-H}}$ bond and the $\text{Cr}-\text{CO}$ bond): (—) main interactions at $\theta = 90^\circ$ and $\theta = 125^\circ$; (---) secondary stabilizing interactions at $\theta = 125^\circ$.

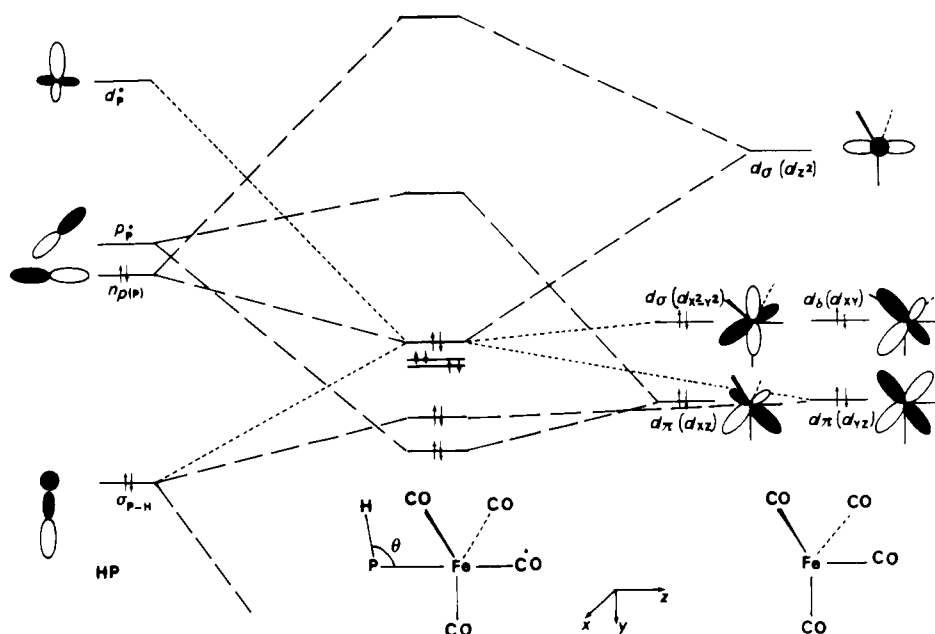


Figure 3. Interaction diagram (EHT) for $\text{HP}=\text{Fe}(\text{CO})_4$ fragments HP, $\text{Fe}(\text{CO})_4$ (HP in axial position): (—) main interactions; (---) secondary interactions.

of HP and the d_{xz} orbital of $\text{Fe}(\text{CO})_4$ (Figure 3).

In the case of an equatorial ligand, the orbitals of the $\text{Fe}(\text{CO})_4$ fragment are considerably modified and are characterized by hybrid LUMO and HOMO orbitals pointing in the direction of the ligand with adequate symmetry to generate interactions with the $n_p(\text{P})$ and $p^*(\text{P})$ orbitals of phosphinidene (Figure 4). This equatorial orientation of the ligand is favored in comparison to an axial one primarily by an increased metal–ligand transfer. The HOMO of the $\text{Fe}(\text{CO})_4$ fragment, a $p-d$ π hybrid, is in fact energetically much higher than the $d_{xz}(\text{Fe})$ orbital previously considered and the only one whose symmetry can lead to an interaction with the $p^*(\text{P})$ orbital. In addition, $p^*(\text{P}), d_{xz}(\text{Fe})$ overlap is much lower than $p^*, d\pi$ hybrid overlap. These two factors contribute to reinforced metal–ligand transfer and are at the origin of a preferred configuration with phosphinidene in an equatorial position.

In both cases considered for $\text{Fe}(\text{CO})_4$, the origins of the observed stabilization by variance of the $\angle\text{HPFe}$ angle from $\theta = 90^\circ$

(maximal $n_p(\text{P}), d_{z^2}$ overlap) to 120° are the same as for $\text{HP}=\text{Cr}(\text{CO})_5$, i.e. stabilizing interactions ($\sigma_{\text{P-H}} \leftrightarrow d_\sigma(\text{Fe}), d\pi(\text{Fe}) \leftrightarrow p-d(\text{P})$ hybrid orbital which is the second virtual orbital of the HP fragment) and the lesser destabilizing interactions.

The comparison of the two entities $\text{HP}=\text{Cr}(\text{CO})_5$ and $\text{HP}=\text{Fe}(\text{CO})_4$ (equatorial ligand) enabled us to observe ligand–metal transfers of about the same order of magnitude and also greater metal–ligand transfer in the case of $\text{Fe}(\text{CO})_4$ than for $\text{Cr}(\text{CO})_5$. (The formation of $\text{HP}=\text{Fe}(\text{CO})_4$ from isolated fragments is thermodynamically favored over that of $\text{HP}=\text{Cr}(\text{CO})_5$).

In terms of the reaction potentialities of these systems, we may note that they are characterized by the last occupied molecular orbital, which includes primarily the $n_p(\text{P})$ pair of the phosphorus atom, and the first virtual orbital involving primarily the $p^*(\text{P})$ orbital. We thus encounter frontier orbitals which are similar to those of noncomplexed phosphinidene. The energy positions of the $\text{HP}=\text{Cr}(\text{CO})_5$ and $\text{HP}=\text{Fe}(\text{CO})_4$ systems are similar, except for a lesser localization on the phosphorus atom in the

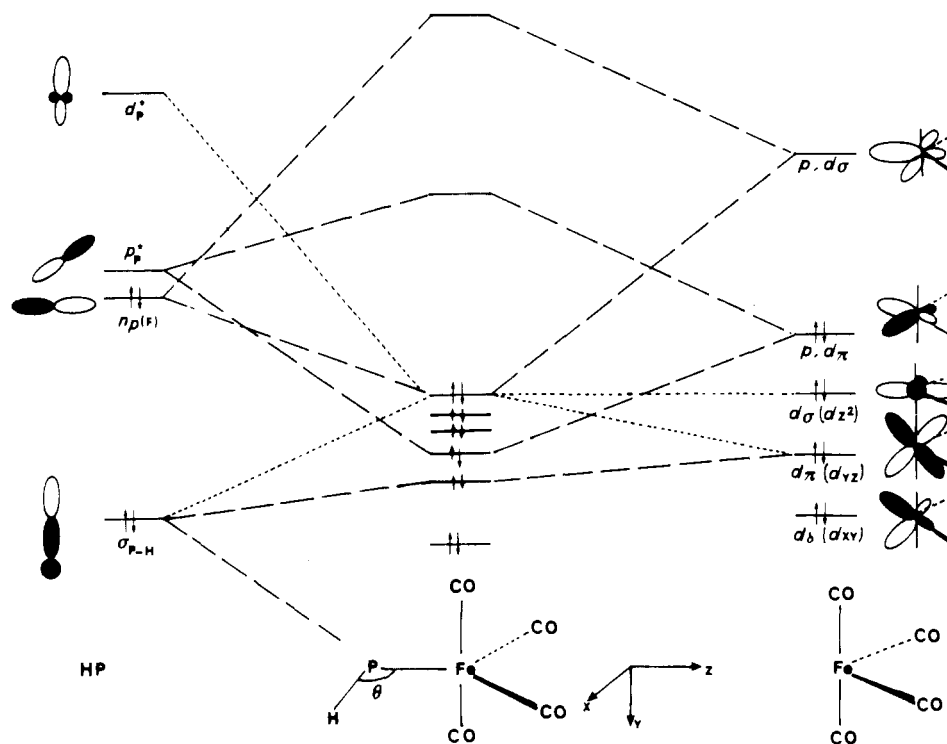


Figure 4. Interaction diagram (EHT) for $\text{HP}=(\text{CO})_4$ fragments HP, $\text{Fe}(\text{CO})_4$ (HP in equatorial position): (---) main interactions; (· · ·) secondary interactions.

LUMO of $\text{Fe}(\text{CO})_4$ than for $\text{Cr}(\text{CO})_5$.

Electronic Structure of the Phosphinidene–Chromium Pentacarbonyl Complex

The behavior of this entity during trapping reactions^{2b} has been compared to that of singlet carbene. In order to verify this hypothesis, we extended our *ab initio* quantum-chemical approach by carrying out calculations on complexed phosphinidene and corresponding fragments by considering the singlet and triplet spin states. In order to be able to utilize the symmetry properties of the system examined in its privileged conformation, we chose, according to the standard options of the PSHONDO program, the Oz axis as the axis of symmetry with the plane xOy thus being the bisecting plane of the Cr–CO bonds (Figure 1).

In the case of phosphinidene, HP, as for its carbene homologue, the results showed the triplet nature of the ground state ($E_{\text{tot}}^{\text{S}} = -6.82931$ au, $E_{\text{tot}}^{\text{T}} = -6.88912$ au). Complexing the HP entity, on the other hand, generated considerable stabilization of the singlet state, which thus appeared to be energetically favored by 52.2 kJ mol⁻¹ in comparison to the triplet state. ($E_{\text{tot}}^{\text{S}} = -122.03291$ au, $E_{\text{tot}}^{\text{T}} = -122.01306$ au). It is to be noted that the calculations were carried out at the simple SCF level without configuration interaction. It is well-known, however that its effect lowers the total valence energy of the singlet state, which can mix with states of the same symmetry, whereas a triplet state is approximately described by a single determinant SCF wave function. The 52.2 kJ mol⁻¹ difference is thus a minimal value of singlet–triplet separation. The ground state of complexed phosphinidene thus corresponds to a singlet state, as predicted during studies of the reactivities of these two entities.^{2c}

Considering the triplet nature of phosphinidene in the ground state, we calculated the triplet state of $\text{Cr}(\text{CO})_5$ with adequate symmetry corresponding to a monooccupation of the d orbital with π symmetry and not of $d\delta$ (HOMO). In this case, complex formation (Figure 5) is equivalent to an electron exchange between the σ and π type monooccupied orbitals of the two fragments.

The $\text{Cr}(\text{CO})_5$ fragment nevertheless presents a singlet type ground state, and the energy difference between this state and the triplet state of $\text{Cr}(\text{CO})_5$ with π symmetry is much greater than that calculated for phosphinidene (≈ 570 kJ mol⁻¹). It would thus seem more reasonable to consider the formation of the phosphinidene complex from the singlet state of the fragments.

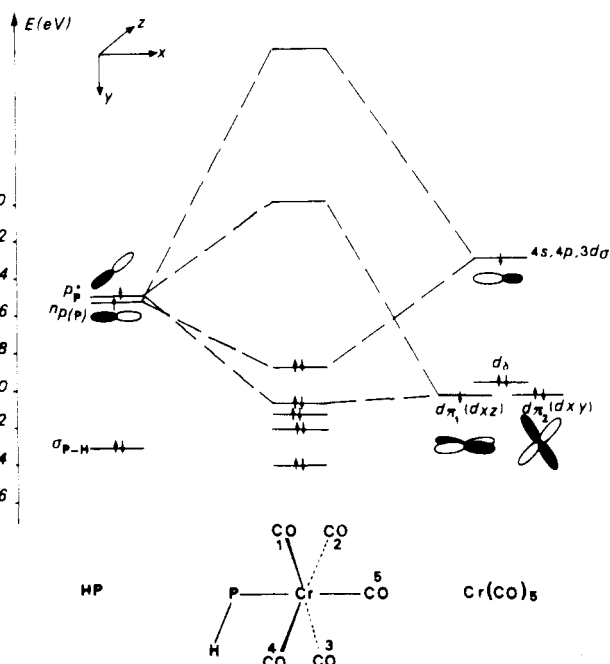



Figure 5. Interaction diagram (*ab initio*) for $\text{HP}=\text{Cr}(\text{CO})_5$ triplet fragments HP and $\text{Cr}(\text{CO})_5$.

Orbital Interaction Diagram. Examination of Figure 6 shows the two principal interactions previously observed in the EHT study.

We can thus distinguish (1) a metal–ligand transfer via the interaction of the HP HOMO ($n_p(\text{P})$) and the $\text{Cr}(\text{CO})_5$ LUMO (hybrid $4s,4p,3d_\sigma$, on chromium), which assures the P–Cr bond in σ and (2) a metal–ligand back-transfer from one of the degenerated $d\pi$ orbitals of $\text{Cr}(\text{CO})_5$, d_{xz} , toward the $p^*(\text{P})$ LUMO of HP, corresponding to the formation of the π bond between the phosphorus and chromium atoms.

The most important secondary interaction is destabilizing, resulting from the geometric structure of the complex. It occurs between the $n_p(\text{P})$ pair of phosphorus and the chromium atom orbital d_{xy} with π symmetry. The orbitals of complexed phos-

Table III. Mulliken Population Analysis: Net Atomic Charges

	Q_P	Q_H	Q_{Cr}	$Q_{C_{1-4}}$	Q_{C_5}	$Q_{O_{1-4}}$	Q_{O_3}	$Q_{C_{6,7}}$	$Q_{H_{6,7}}$
HP	-0.05	+0.05							
Cr(CO) ₅			+0.81	+0.22	+0.21	-0.38	-0.38		
HPCr(CO) ₅	+0.41	+0.02	+0.37	+0.19	+0.23	-0.36	-0.35		
	+0.57	+0.06	+0.27	+0.18	+0.23	-0.37	-0.37	-0.13	+0.13

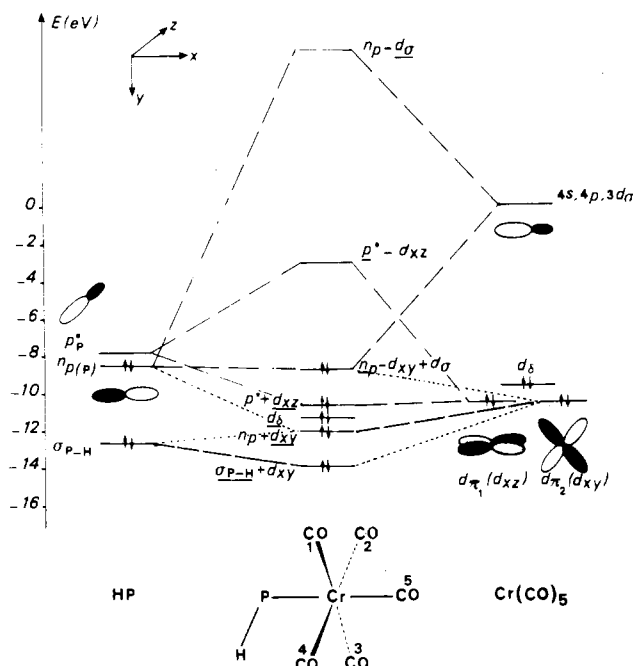


Figure 6. Interaction diagram (ab initio) for $HP=Cr(CO)_5$, singlet fragments HP and $Cr(CO)_5$ (underlined values correspond to the highest localizations): (—) main interactions; (---) secondary interactions.

phosphinidene are characterized by a last occupied orbital with a predominant participation by the $n_p(P)$ pair of phosphorus; the following three occupied orbitals ($d\pi_1$, $d\delta$, $d\pi_2$) are localized primarily on the d orbitals of chromium. An orbital appears at lower energies which involves primarily the σ_{P-H} bond. Finally, the LUMO of this system is considerably localized on the phosphorus atom (p^* orbital). We thus have frontier orbitals in complexed phosphinidene that are of the same type as those of singlet phosphinidene, HP. From an energy standpoint, the HOMO is only slightly stabilized by complexing, but we note a rather considerable destabilization of the LUMO. The present results suggest that if the reactivity of singlet phosphinidenes and metal phosphinidene complexes is frontier orbital controlled, then the behavior of these species with alkenes must be quite similar.

Charge Distributions. In addition, a Mulliken population analysis performed on the HP, $Cr(CO)_5$, and $HP=Cr(CO)_5$ systems enabled us to define the degree of the existing transfers. First, the decreased electronic charge on the d_{xz} orbital of the chromium atom (1.648 in $Cr(CO)_5$ and 1.160 in $HP=Cr(CO)_5$) corresponds to a metal–ligand transfer on the order of $0.49 e^-$. (An absolute quantitative value should not be attributed to these figures because of the well-known influence of the basis set used on the Mulliken populations.) In parallel, we were able to estimate the ligand–metal transfer via the $n_p(P)/4s, 4p, 3d\sigma(Cr)$ interaction at about $0.95 e^-$. It thus appears that there is much more σ transfer than π transfer.

The positive charge of the chromium atom in $HP=Cr(CO)_5$, which has gained electrons, decreases in comparison to that in $Cr(CO)_5$ (Table III). On the other hand, the effect of complexing imparts a notable net positive charge of +0.41 to phosphorus. The π gain in this atom does not compensate its considerable σ loss. In comparison to carbene complexes,¹⁶ phosphinidene complexes thus seem much more electropositive, a hypothesis formulated previously.^{2b}

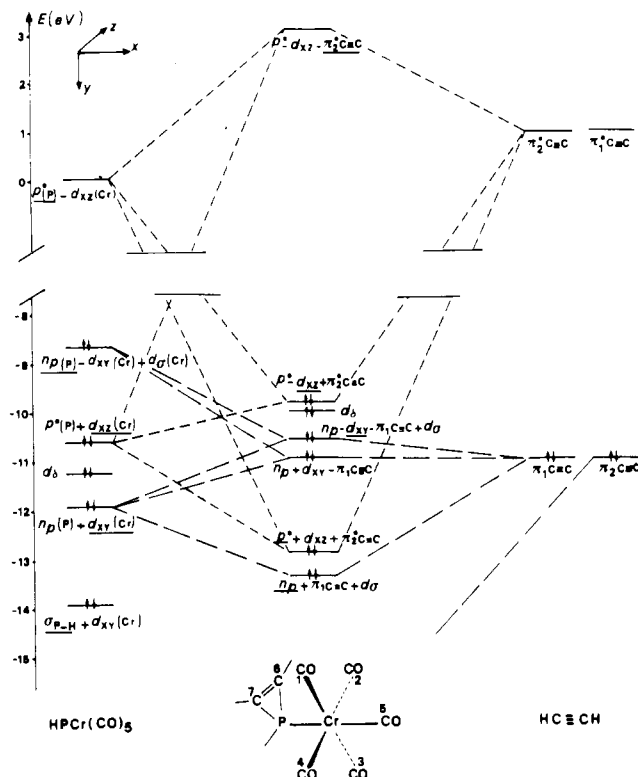


Figure 7. Interaction diagram (ab initio) for $HP=Cr(CO)_5$ fragments $HP=Cr(CO)_5$ and $H-C\equiv C-H$ (underlined values correspond to the highest localizations): (—) interactions with $n_p(P)$; (---) interactions with $p^*(P)$.

Phosphorus in the isolated phosphinidene is charged by -0.05 . Thus, the reactivity of phosphinidene–metal complexes could be explained as charge controlled rather than frontier orbital controlled. These results were consistent with the conclusions of Casey¹⁷ and Brookhart,¹⁸ who pointed out the relative reactivity of alkenes toward metal–carbene complexes can be understood in terms of an initial interaction between the electrophilic carbene carbon atom and one extremity of the alkene.

Electronic Structure of the Phosphirene–Chromium Pentacarbonyl Complex

We continued the present investigation by examining the phosphirene–chromium pentacarbonyl complex, a stable compound obtained by trapping the corresponding complexed phosphinidene with acetylene.

Orbital Interaction Diagram. In order to more fully understand the stabilization of this system, we examined the interactions between the orbitals of the fragments $H-C\equiv C-H$ and $HP=Cr(CO)_5$ (Figure 7).

Two principal interactions can be distinguished: the first is a destabilizing interaction between the $n_p(P)$ pair of phosphorus and the acetylene orbital with π symmetry ($\pi_1(C\equiv C)$). This orbital nevertheless involves the d_{xy} (occupied) and $d\sigma$ (virtual) orbitals of chromium. This six-electron interaction is thus delocalized on

(17) Casey, C. P.; Polichnowski, S. W.; Shusterman, A. J.; Jones, C. R. *J. Am. Chem. Soc.* **1979**, *101*, 7282.

(18) Brookhart, M.; Humphrey, M. B.; Kratzer, H. J.; Nelson, G. O. *J. Am. Chem. Soc.* **1980**, *102*, 7802.

chromium, phosphorus, and acetylene and generates three molecular orbitals. In agreement with orbital mixing rules¹⁹ and with the energy position of $\pi_1(\text{C}\equiv\text{C})$ in relation to the combinations $n_p(\text{P}) - d_{xy}(\text{Cr}) + d\sigma(\text{Cr})$, $n_p(\text{P}) + d_{xy}(\text{Cr})$ taken into account, the totally antibonding orbital is localized primarily on the $d_{xy}(\text{Cr})$ orbital and the lowest totally bonding orbital is on the $n_p(\text{P})$ pair. The intermediate orbital, on the other hand, has similar localizations on $n_p(\text{P})$, $d_{xy}(\text{Cr})$, and $\pi_1(\text{C}\equiv\text{C})$.

The second is an interaction involving the $p^*(\text{P})$ orbital of complexed phosphinidene and the vacant acetylene orbital with adapted symmetry $\pi^*_2(\text{C}\equiv\text{C})$. In this case as well, it should be noted that the $p^*(\text{P})$ orbital interacted with the occupied chromium d_{xz} orbital in complexed phosphinidene. The localizations of these three molecular orbitals of complexed phosphirene can be deduced with the above-mentioned rules. The highest one is a virtual orbital of the mixed system $p^*(\text{P})$, $d_{xz}(\text{Cr})$, and primarily $\pi^*_2(\text{C}\equiv\text{C})$; the next (HOMO of complexed phosphirene) corresponds to a considerable weighting of the $d_{xz}(\text{Cr})$ orbital. Finally, the lowest is characteristic of the $p^*(\text{P})$ orbital, albeit with a nonnegligible participation of the $d_{xz}(\text{Cr})$ orbital. At the level of this $p^*(\text{P}) \leftrightarrow \pi^*_2(\text{C}\equiv\text{C})$ interaction, it is worthwhile to compare the respective positions of the $p^*(\text{P})$ orbitals in phosphinidene and in complexed phosphinidene (Figure 6). The much higher energy of this orbital in the latter system implies a greater interaction with $\pi^*_2(\text{C}\equiv\text{C})$, reflected by a much lower energy of the molecular orbital describing the antisymmetric combination of P–C bonds (-10.95 eV in phosphirene,²⁰ -12.86 eV in the phosphirene complex). We thus have a direct stabilizing effect by complexing.

Charge Distributions. Based on these interactions, we can explain the charge transfers observed between the phosphorus atom and the metal. The n_p pair of phosphorus is delocalized toward the acetylene system ($\pi_1(\text{C}\equiv\text{C})$) with lesser transfer toward chromium in σ . Similarly, the delocalization of $p^*(\text{P})$ on the acetylenic system induces a much weaker π transfer of chromium toward phosphorus. This is equivalent to a weakening of the P–Cr bond, in σ and especially in π .

Thus, the chromium atom has a net positive charge ($Q_{\text{Cr}} = +0.27$) which is lower than that in complexed phosphinidene ($Q_{\text{Cr}} = +0.37$). The phosphorus atom, on the other hand, is more positive ($Q_{\text{P}} = +0.57$) than in complexed phosphinidene ($Q_{\text{P}} = +0.41$).

Stabilization of Phosphirene by Complexation. In order to define the effect of complexing on the stabilization of the phosphirene, we analyzed the interaction diagram phosphirene \leftrightarrow $\text{Cr}(\text{CO})_5$ (Figure 8). We note the following:

(1) There is a modification of the destabilizing interaction $n_p(\text{P}) \leftrightarrow \pi_1(\text{C}\equiv\text{C})$ by mixing with the occupied $d\pi$ ($d_{xy}(\text{Cr})$) orbital. In the context of a strong "system $\pi \leftrightarrow$ lone pair" interaction this is reflected by a loss of the "lone pair" character. In addition, we observed a stabilizing interaction with the LUMO ($4s, 4p, 3d\sigma$) of the $\text{Cr}(\text{CO})_5$ fragment, also responsible for the stabilization of the orbitals involved. The antiaromatic character of phosphirene is thus attenuated by complexing ($n_p(\text{P}) \rightarrow$ Cr transfer).

(2) There is a stabilization of the characteristic orbital of P–C bonds by the mixing of the d_{xz} orbital of chromium with $p^*(\text{P})$ and $\pi^*_2(\text{C}\equiv\text{C})$. The resulting metal–phosphorus transfer causes a greater phosphorus–acetylene system delocalization, resulting in stronger P–C bonds.

Thus, even though the P–Cr is weakened, there remains an obvious stabilization effect during complexing, arising from a participation of the metal in the two phenomena governing the stability of the phosphirene ring: (1) a decrease of the lone-pair character of phosphorus and thus the antiaromaticity (less pyramidalization); (2) an increase of σ delocalization, which is in good agreement with the slight decrease of the P–C bond lengths and increase of the C=C bond length.

In parallel to this theoretical study, we recorded the photoelectron spectra of these complexes. This technique is well suited for the estimation of metal–ligand interactions and also led to the

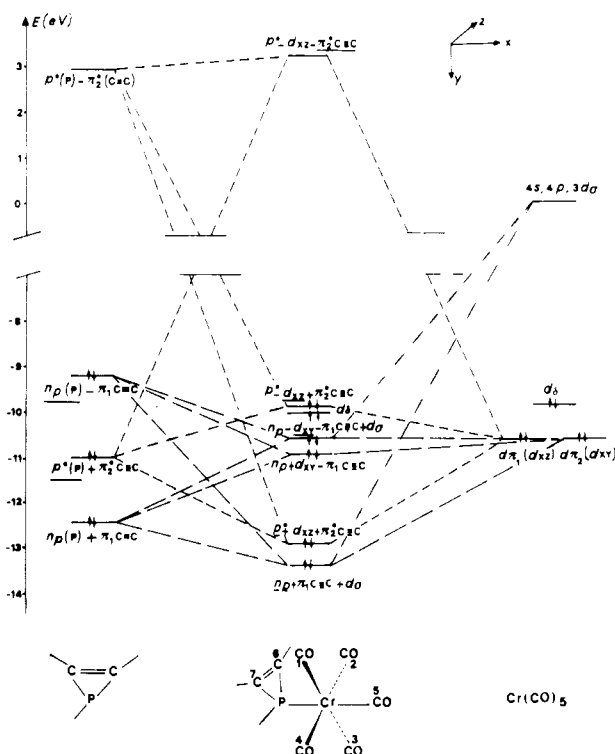
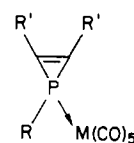


Figure 8. Interaction diagram (ab initio) for phosphirene– $\text{Cr}(\text{CO})_5$, fragments phosphirene and $\text{Cr}(\text{CO})_5$ (underlined values correspond to the highest localizations): (—) interactions with $n_p(\text{P})$; (---) interactions with $p^*(\text{P})$.

verification of the validity of our conclusions on the origin of the stabilization brought about by complexing.

Photoelectron Spectra of Phosphirene Complexes. In the conditions of temperature (more than 100°C) and pressure (5×10^{-2} mbar) required for recording the spectra, these complexes degrade with the formation of the corresponding acetylenic derivatives.

Only the spectra of



- 1: $\text{M} = \text{W}$, $\text{R}' = \text{Et}$, $\text{R} = \text{Me}$
 2: $\text{M} = \text{W}$, $\text{R}' = \text{Et}$, $\text{R} = \text{Ph}$
 3: $\text{M} = \text{Cr}$, $\text{R}' = \text{Et}$, $\text{R} = \text{Ph}$

were analyzed and are shown in Figures 9–11.

In addition to the ionization of d electrons, we expect three ionizations of these compounds between 9 and 12 eV. The high intensity of the 10.60-eV band of **1** suggests the overlap of two bands. The bands at 9.1 and 11.75 eV thus arise from slight degradation with the formation of diethylacetylene. In the cases of **2** and **3** we cannot exclude the presence of the acetylenic derivative, since the first band could be masked under the 9-eV band, corresponding to ionizations of the phenyl ring of the complex. These compounds nevertheless appear to decompose with more difficulty, since we see no truly intense band in the 11.75-eV region. Ionization potentials are reported in Table IV.

Compound 1. When passing from He I to He II (Figure 9a,b), we see an unmistakable intensity increase of the first band, which is attributed to the ionization of the d electrons of the metal. The expansion of this first band (Figure 9c) clearly shows the appearance of three separate ionizations. The intensities of the bands at 9.87 and 10.60 eV decrease, however, especially that at 10.60 eV.

Table V contains the ionization potentials calculated for this molecule, taking into account polarization and loss of interpair correlation corrections to Koopmans' theorem. We have also listed

(19) Inagaki, S.; Fujimoto, H.; Fukui, K. *J. Am. Chem. Soc.* **1976**, *98*, 4054.
 (20) Gonbeau, D.; Pfister-Guillouzo, G. *Nouv. J. Chim.*, in press.

Table IV. Experimental Vertical Ionization Potentials (eV) of Phosphirene Complexes^a

Complex	IP (eV)
1-methylphosphirene (W)	7.35
	7.70
	9.87
1-methylphosphirene (Cr)	7.30
	7.50
	7.80
1-methylphosphirene (Cr)	7.20
	7.50
	8.9 - 9.3
Phosphirene (W)	9.
	10.30
	10.75
Phosphirene (Cr)	10.20
	10.65
	11.35
Phosphirene (Cr)	11.35
	10.60
	11.35

^a Large (small) downward-pointing arrows indicate that the intensity of the band decreases strongly (weakly) when going from the He I to He II spectrum. Large upward-pointing arrows indicate that the intensity of the band increases strongly when going from the He I to the He II spectrum.

the ionization potentials calculated for phosphirene and 1-methylphosphirene in order to estimate the effect of methylation on the phosphorus.

As we deduced from the intensity variations, the first band corresponds to d-electron ionizations. Considering the polarization corrections, known to be considerable for d electrons, the calculated values correctly reflect the experimentally observed ionization potentials for which the order is $d\pi$, $d\delta$, $d\pi$. The band at 9.87 eV is attributed to the molecular orbital primarily corresponding to the $n_p(\text{P}) \leftrightarrow \pi(\text{C}=\text{C}) \leftrightarrow d_{xy}(\text{M})$ interaction with, as we have seen above, a nonnegligible weighting of d orbitals and a weak localization on phosphorus. This attribution is consistent with the slight intensity variation observed during the He I/He II shift.

Two ionizations are attributed to the 10.60-eV band: that of the characteristic molecular orbital of the P-C bonds constructed from the virtual orbitals of phosphorus and acetylene, with a notable participation of the d_{xz} orbital; that corresponding to the phosphorus pair ethylenic system interaction. The localization calculated for phosphorus is considerable, but in this case there is relatively little participation by d orbitals. The considerable intensity decrease observed for this band is highly consistent with this attribution.

Taking alkyl group effects into account for the phosphorus and ethylene bond, we note that the ionization potentials calculated for the nonsubstituted molecule are not in good agreement with the experimental data. The probable cause is the fact that specific correlation effects of the ion were not included in our calculations. These systems in fact present vacant orbitals with very low energies (with π and σ symmetry), and thus this effect should be great.^{12c}

Compounds 2 and 3. In addition to the intense band at about 9 eV due to the ionizations of the phenyl ring, three distinct bands are seen between 10.20 and 11.35 eV. The presence of the phenyl ring induces a stabilization of the two ionizations associated with the $n_p(\text{P}) \leftrightarrow \pi(\text{C}=\text{C}) \leftrightarrow d_{xy}(\text{M})$ interaction at 10.30–11.35 (2)

Table V. Calculated Ionization Potentials (eV): Phosphirene and Phosphirene Complex

phosphirene		1-methylphosphirene		phosphirene complex				
IP(Koopmans) (assign)	IP(cor)	IP- (Koopmans)	IP(cor)	IP(Koopmans) (assign)	polarizn	correln	IP(cor)	IP- (exptl) ^a
9.13	9.10	8.61	8.48	9.84 ($d_{\pi}(\text{Cr})$)	2.32	-0.35	7.87	7.35 7.70
				9.87 ($d_{\delta}(\text{Cr})$)	2.62	-0.53	7.77	
				10.43 ($d_{\pi}(\text{Cr})$)	2.36	-0.32	8.39	
				10.72	1.10	-0.21	9.88	9.87
				($n_p(\text{P}) - \pi(\text{C}=\text{C})$)				
10.95 ($\sigma(\text{P}-\text{C})$)	10.77	10.77	10.51	12.86 ($\sigma(\text{P}-\text{C})$)	0.82	-0.16	12.20	10.60
12.29	12.00	11.83	11.53	13.31	0.88	-0.19	12.62	
				($n_p(\text{P}) + \pi(\text{C}=\text{C})$)				
14.40	14.14	13.76	13.40	15	0.55	-0.11	14.57	12.55

^a Compound 1.

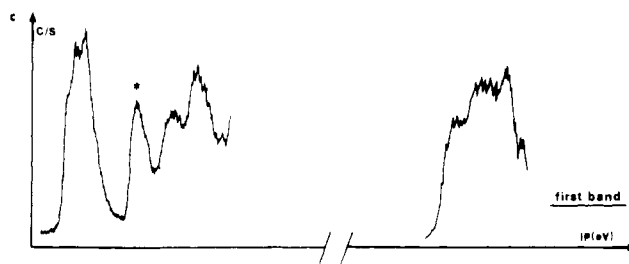
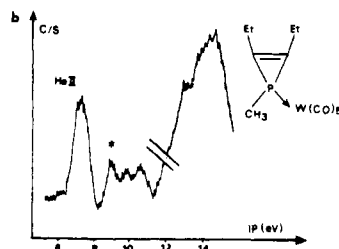
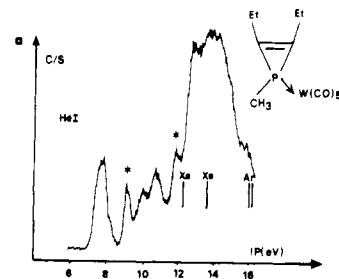


Figure 9. Photoelectron spectra of compound 1 (asterisks denote bands of $\text{Et}-\text{C}=\text{C}-\text{Et}$): (a) He I spectrum; (b) He II spectrum; (c) expanded scale of the first band.

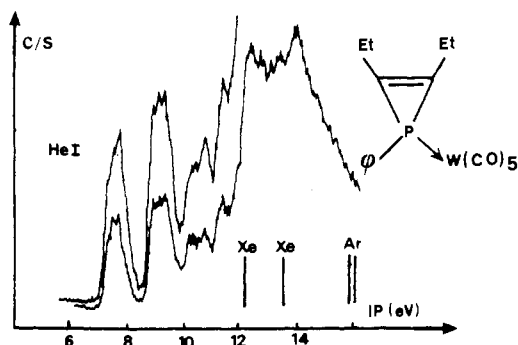


Figure 10. Photoelectron spectra (He I) of compound 2.

and 10.20–11.35 eV (3), respectively. The ionization potentials observed at 10.75 and 10.65 eV correspond to the molecular orbital with σ symmetry, a combination of the p^* orbitals of phosphorus,

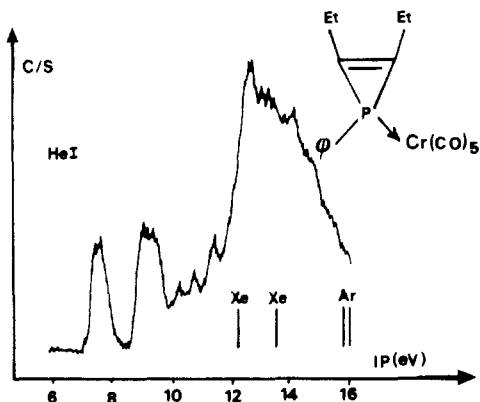


Figure 11. Photoelectron spectrum (He I) of compound 3.

the $\pi^*(\text{C}\equiv\text{C})$ orbital of acetylene, and the d_{xz} orbital of the metal.

This attribution is supported by two experimental observations. The band at 11.35 eV in these two compounds is that whose intensity decreases the greatest (localization on phosphorus). Also when passing from tungsten to chromium, we note that the first band and the two bands at 10.30 and 10.75 eV, previously attributed to the ionization of molecular orbitals with a certain degree of localization of the d orbitals of the metal, shift toward lower energies.

On the basis of these experimental data, we observe a destabilizing "lone pair $n_p-\pi(\text{C}=\text{C})$ system" interaction of about 1 eV, which does not seem to be considerable. The ionization potential associated with the most characteristic orbital of these entities, since it partially reflects their stabilization, is nevertheless quite high at 10.60–10.75 eV. In nonsubstituted phosphirane, the ionization potential associated with the orbital partially presenting the same characteristics (nonparticipation of the d orbitals of the metal) appears at 10.21 eV,²¹ reflecting a considerable overall stabilization, taking alkyl group effects into account.

Conclusion

We have investigated the electronic structures of complexes of phosphinidene and phosphirene. The existence of the former

was presumed by the identification of their trapping products. Using an EHT approach, we have proposed a preferential structure for complexes of phosphinidene with $\text{Cr}(\text{CO})_5$ and $\text{Fe}(\text{CO})_4$. It is interesting to note that the spatial distribution of the P–R moiety in the complex with $\text{Cr}(\text{CO})_5$ is comparable to experimental data obtained with the acetylenic trapping product of the complex with $\text{W}(\text{CO})_5$, i.e. an $\angle\text{MPR}$ angle of 125° and the P–R bond in the bisecting plane of the CO groups.

Using ab initio calculations, we verified that the ground state of this complex is singlet, a hypothesis previously postulated for interpreting its chemical behavior.

Phosphinidene–metal and metal–phosphinidene charge transfers have been discussed in relation to an orbital interaction diagram. They correspond to a highly electropositive complexed phosphinidene entity.

The formation of stable phosphirene complexes is an exciting problem, since the origin of the stabilization of these antiaromatic systems remains a subject of discussion. We have extended our quantum-chemical approach with an analysis of PES spectra. Thus, in spite of a weakening of the P–Cr bond, electron-transfer analyses show the important role played by the metal atom in the antiaromaticity of the system and in the σ delocalization.

These two phenomena, responsible for the stabilization of the complexed phosphirene system, were experimentally demonstrated with PES. The spectra showed two IP's associated with the MO delocalized on the lone pair of phosphorus and the ethylene π system, with a slight energy difference, and a well-stabilized IP corresponding to the P–C bonds of the ring.

Acknowledgment. The authors thank Dr. J. C. Barthelat (Laboratoire de Physique Quantique, Toulouse, France) for his help in the determination of the pseudopotential for chromium and F. Gracian for her technical assistance in the recording of spectra. We thank the Centre de Calcul Vectoriel pour la Recherche, Ecole Polytechnique, Palaiseau, France, for generous allotments of computer time (ATP Cray 1983).

Registry No. 1, 82281-50-3; 2, 82265-69-8; 3, 97704-82-0; $\text{HP}=\text{Cr}(\text{CO})_5$, 98482-23-6; $\text{HP}=\text{Fe}(\text{CO})_4$, 98482-24-7; phosphirene–chromium pentacarbonyl complex, 98482-25-8.

Supplementary Material Available: Listings of the Gaussian valence basis set (Table I) and pseudopotential parameters (Table II) (2 pages). Ordering information is given on any current masthead page.

(21) Aue, D. H.; Webb, H. M.; Davidson, W. R.; Vidal, M.; Bowers, M. T.; Goldwhite, H.; Vertal, L. E.; Douglas, J. E.; Kollman, P. A.; Kenyon, G. L. *J. Am. Chem. Soc.* **1980**, *102*, 5151.